Heliyon 10 (2024) e26326

Contents lists available at ScienceDirect

Heliyon

journal homepage: www.cell.com/heliyon

Research article

# Lipidomics based on UHPLC/Q-TOF-MS to characterize lipid metabolic profiling in patients with newly diagnosed type 2 diabetes mellitus with dyslipidemia

Xunlong Zhong [a,1], Chang Xiao [a,1], Ruolun Wang [a], Yunfeng Deng [a], Tao Du [b], Wangen Li [b], Yanmei Zhong [c,**], Yongzhen Tan [d,*]

[a] Department of Pharmacy, the Second Affiliated Hospital of Guangzhou Medical University, Guangzhou, 510260, China
[b] Department of Endocrinology, the Second Affiliated Hospital of Guangzhou Medical University, Guangzhou, 510260, China
[c] New Drug Research and Development Center, Guangdong Pharmaceutical University, Guangzhou, 510006, China
[d] Department of Traditional Chinese Medicine, the Second Affiliated Hospital of Guangzhou Medical University, Guangzhou, 510260, China

ARTICLE INFO

*Keywords:*
Lipid profiles
Type 2 diabetes mellitus with dyslipidemia
Hyperlipidemia
UHPLC-MS
Lipidomics

ABSTRACT

Dyslipidemia often accompanies type 2 diabetes mellitus (T2DM). Elevated blood glucose in patients commonly leads to high levels of lipids. Lipid molecules can play a crucial role in early detection, treatment, and prognosis of T2DM with dyslipidemia. Previous lipid studies on T2DM mainly focused on Western diabetic populations with elevated blood glucose. In this research, we investigate both high blood sugar and high lipid levels to better understand changes in plasma lipid metabolism in newly diagnosed Chinese T2DM patients with dyslipidemia (NDDD). We used a plasma lipid analysis method based on ultra-high performance liquid chromatography coupled with mass spectrometry technology (UHPLC-MS) and statistical analysis to characterize lipid profiles and identify potential biomarkers in NDDD patients compared to healthy control (HC) subjects. Additionally, we examined the differences in lipid profiles between hyperlipidemia (HL) patients and HC subjects. We found significant changes in 15 and 23 lipid molecules, including lysophosphatidylcholine (LysoPC), phosphatidylcholine (PC), phosphatidylethanolamine (PE), sphingomyelin (SM), and ceramide (Cer), in the NDDD and HL groups compared to the HC group. These altered lipid molecules are associated with five metabolic pathways, with sphingolipid metabolism and glycerophospholipid metabolism being the most relevant to glucose and lipid metabolism changes. These lipid biomarkers are strongly correlated with traditional markers of glucose and lipid metabolism. Notably, Cer(d18:1/24:0), SM(d18:1/24:0), SM(d18:1/16:1), SM (d18:1/24:1), and SM(d18:2/24:1) were identified as essential potential biomarkers closely linked to clinical parameters through synthetic analysis of receiver operating characteristic curves, random forest analysis, and Pearson matrix correlation. These lipid biomarkers can enhance the risk prediction for the development of T2DM in individuals with dyslipidemia but no clinical signs of high blood sugar. Furthermore, they offer insights into the pathological mechanisms of T2DM with dyslipidemia.

* Corresponding author.
** Corresponding author.
*E-mail addresses:* zhongyanmei33@163.com (Y. Zhong), gzzyms0421@163.com (Y. Tan).
[1] These authors are co-first authors.

https://doi.org/10.1016/j.heliyon.2024.e26326
Received 30 January 2024; Accepted 12 February 2024
Available online 13 February 2024

**Abbreviations**

| | |
|---|---|
| T2DM | type 2 diabetes mellitus |
| IR | insulin resistance |
| NDDD | newly diagnosed T2DM with dyslipidemia |
| HL | hyperlipidemia |
| HC | healthy controls |
| HbA1c | hemoglobin A1c |
| FPG | fasting plasma glucose |
| 2hPBG | 2 h postprandial blood glucose |
| CHOL | total cholesterol |
| LDL-C | low-density lipoprotein cholesterol |
| TG | triglycerides |
| HDL-C | high-density lipoprotein cholesterol |
| apoB | apolipoprotein B |
| ALT | alanine aminotransferase |
| AST | aspartate aminotransferase |
| CREA | creatinine |
| UHPLC/Q-TOF-MS | ultra-high performance liquid chromatography coupled with quadrupole-time-of-flight mass spectrometry |
| QC | quality control |
| PCA | principal component analysis |
| OPLS-DA | orthogonal projection discriminate analysis |
| RPT | response permutation testings |
| VIP | variable importance in projection |
| FC | fold change |
| ROC | receiver operator characteristic |
| AUC | area under the curve |
| LysoPC | lysophosphatidylcholine |
| PC | phosphatidylcholine |
| PE | phosphatidylethanolamine |
| SM | sphingomyelin |
| Cer | ceramide |
| RF | random forest |
| MDA | mean decrease accuracy |
| FFAs | free fatty acids |
| GPs | glycerophospholipids |
| PLA2 | phospholipase A2 |
| ERS | endoplasmic reticulum stress |
| SREBP-1c | sterol regulatory element binding protein 1c |
| ChREBP | carbohydrate response element binding protein |
| LXRα | liver X receptor |

## 1. Introduction

Diabetes comprises a group of conditions affecting glucose metabolism, characterized by either a deficiency in insulin secretion or insulin resistance (IR), often accompanied by disturbances in lipid and protein metabolism. By the year 2045, an estimated 783.2 million people worldwide will be living with diabetes, with China alone accounting for 174 million cases, the majority of which will be type 2 diabetes mellitus (T2DM) [1]. In China, the prevalence of T2DM among adults stands at 11.6%, and an additional 50.1% have pre-diabetic conditions [2]. T2DM is marked by its protracted course, a multitude of complications, and complex clinical manifestations [3].

Presently, the diagnosis of T2DM primarily relies on clinical symptoms and blood glucose levels. Nonetheless, roughly 59% of early-stage diabetic patients might experience misdiagnosis or evade detection through fasting plasma glucose (FPG) assessments [4]. This holds considerable clinical importance as it frequently leads to missed opportunities for intervention during the initial onset of symptoms. Furthermore, conventional thinking held that T2DM was primarily a disorder of glucose metabolism, with subsequent lipid metabolism irregularities. However, contemporary research indicates that these two disorders often develop concurrently. Pre-diabetes is frequently accompanied by varying degrees of excess weight or obesity, along with dyslipidemia, and over 50% of T2DM patients exhibit evident dyslipidemia [5–7]. Lipids possess biological functions and participate in energy transfer, cellular signaling, growth, development, division, differentiation, and apoptosis. A comprehensive exploration of lipidomics investigates the intricate interplay between lipid metabolism disorders and T2DM, with the identification of lipid biomarkers offering valuable insights

into the pathogenesis, early detection, and treatment of T2DM in individuals with dyslipidemia.

In contrast to traditional lipid profiling, lipidomics, utilizing ultra-high performance liquid chromatography-tandem mass spectrometry (UHPLC-MS), enables the simultaneous qualitative characterization of various lipid species, offering a comprehensive insight into lipid metabolism. Recent literature has extensively documented variations in lipid profiles between individuals with T2DM and their healthy counterparts [8–11]. These studies have underscored the significant correlation between lipid metabolism and glucose regulation. However, the bulk of research on the pathogenesis and identification of lipid biomarkers for T2DM, based on plasma metabolite analysis, has primarily focused on Western populations. There is a notable scarcity of research on predictive lipid metabolites for newly diagnosed T2DM within diverse ethnic groups, particularly in Asian populations. Moreover, there is a limited understanding of the relationship between lipid metabolites and T2DM within different regions of China characterized by varying dietary patterns. Furthermore, most studies have targeted T2DM patients with only elevated blood glucose levels, with limited attention given to those with concurrent dyslipidemia. As previously highlighted, dyslipidemia is a prevalent comorbidity of T2DM, and it is essential to consider both conditions holistically.

In this study, we conducted a comprehensive examination of blood lipid alterations in individuals with T2DM-related dyslipidemia and hyperlipidemia, comparing them with healthy subjects. Our objective was to employ a lipidomic approach to pinpoint potential lipid biomarkers and metabolic pathways. This research aims to enhance our understanding of the risk assessment and pathological mechanisms associated with T2DM complicated by dyslipidemia, ultimately facilitating the development of effective preventive and therapeutic strategies tailored to Chinese patients with T2DM-related dyslipidemia.

## 2. Materials and methods

### 2.1. Reagents and Chemicals

MS-grade acetonitrile, methanol, and isopropanol were procured from Merck (Shanghai, China). HPLC-grade formic acid was provided by ANPEL Laboratory Technologies (Shanghai) Inc. Analytical reagent chloroform and ammonium formate were sourced from Damao Chemical Reagent Factory (Tianjin, China). Leucine-enkephalin was supplied by Sigma-Aldrich (Steinheim, Germany). Double-distilled water was obtained from Watson's Food & Beverage (Guangzhou, China). Reference standards, including LysoPC (18:0/0:0) and LysoPC (18:1/0:0), were purchased from Avanti Polar Lipids Inc.

### 2.2. Study subjects

Participants were recruited from the Second Affiliated Hospital of Guangzhou Medical University, Guangdong Province, between August 2019 and October 2019. The study encompassed patients with newly diagnosed type 2 diabetes mellitus and dyslipidemia (NDDD), those with hyperlipidemia (HL), and healthy controls (HC). Prior hypoglycemic or lipid-lowering treatments had not been administered to any NDDD or HL participants. Selection of HC subjects was carried out from the physical health outpatient clinic, and they did not meet the criteria for treatment of hypoglycemia or hypolipidemia.

Diagnoses of glucose and lipid metabolism disorders were primarily based on criteria established by the World Health Organization (WHO), the International Diabetes Federation (IDF), the China Cholesterol Education Program (CCEP), and the Chinese Diabetes Society (CDS) [12]. Criteria encompassed HbA1c levels $\geq$6.5%, FPG levels $\geq$7.0 mmol/L, or 2-h postprandial (after breakfast) blood glucose (2hPBG) levels $\geq$11.1 mmol/L. Moreover, lipid metabolism disorder indicators included CHOL levels $\geq$5.2 mmol/L, LDL-C levels $\geq$3.4 mmol/L, or TG levels $\geq$1.7 mmol/L. Confirmation necessitated that these parameters be tested on at least two occasions.

Exclusionary criteria include: Patients currently undergoing hypoglycemic and lipid-lowering treatment. Patients with diabetes complications, such as diabetic nephropathy, diabetic retinopathy, and diabetic peripheral neuropathy. Patients diagnosed with type 1 diabetes and gestational diabetes. Patients using medications that may induce elevated blood sugar or blood lipid levels. Patients with coexisting diseases or a history of surgeries. Patients aged below 18 or above 70 years. Patients experiencing liver and kidney dysfunction.

All experiments received approval from the Medical Ethics Committee of the Second Affiliated Hospital of Guangzhou Medical University (Approval No: 2020-hs-07). The implementation adhered to the fundamental principles outlined in the Declaration of Helsinki.

### 2.3. Data collection

Demographic information, including age and gender, and biochemical parameters such as FPG, CHOL, TG, LDL-C, high-density lipoprotein cholesterol (HDL-C), HbA1c, apoB, alanine aminotransferase (ALT), aspartate aminotransferase (AST), and creatinine (CREA), were obtained and recorded.

### 2.4. Sample preparation

The extraction and separation of lipids from plasma were carried out using a combination of the Folch and Bligh & Dyer methods. A mixture of chloroform and methanol (1.5 mL, 2:1, v/v) was added to a 150 μL plasma sample. The mixture was vortex-mixed and allowed to settle for approximately 3 min. Subsequently, 500 μL of distilled water was introduced. The mixtures were vortex-mixed for 1 min and left to rest at room temperature for 5 min. Following this, the solutions were centrifuged at 12,000 rpm for 10 min at 4 °C.

The lower organic phase was carefully extracted and dried using nitrogen. The resulting residue was reconstituted with 500 μL of acetonitrile/isopropanol (1:1, v/v) containing 10 mM ammonium formate and centrifuged at 12,000 rpm for 10 min. A 300-μL aliquot of the supernatant was employed for ultra-high performance liquid chromatography coupled with quadrupole-time-of-flight mass spectrometry (UHPLC/Q-TOF-MS) analysis.

### 2.5. Chromatographic and mass spectrometric conditions

For the analysis, the Waters ACQUITY UHPLC™ instrument, manufactured by Waters in Milford, USA, was employed. The system was comprised of a quaternary pump, vacuum degasser, and an autosampler. Chromatographic peaks were separated on a UPLC™ BEH C18 column (50 mm × 2.1 mm, 1.7 μm, Waters, USA), with the column temperature being maintained at 50 °C. A gradient elution system was utilized, consisting of (A) 10 mM ammonium formate with 0.1% formic acid in water and (B) 10 mM ammonium formate with 0.1% formic acid in acetonitrile/isopropanol (1:1, v/v). The following conditions were employed: 0–4 min, during which the composition of B ranged from 61% to 81.4%, 4–5 min with B at 81.4%–82%, 5–8 min with B at 82%, 8–9 min with B at 82%–83%, 9–12 min with B at 83%–83%, 12–15 min with B at 83%–95%, 15–16 min with B at 95%–99%, 16–17 min with B at 99%–100%, and 17–22 min with B at 100%. The flow rate was set at 0.30 mL/min, and an injection volume of 5 μL was utilized.

In this experiment, the Waters mass spectrometer was utilized. It was equipped with an electrospray ion source and operated in positive ion mode, capturing full scan mass data within the *m/z* range of 100–1500 Da. The ion source temperature was established at 100 °C, with a cone gas flow of 50 L/h. The desolvation temperature was maintained at 300 °C, with a gas flow of 500 L/h. The capillary voltage was set at 3.0 kV, and the sample cone voltage was adjusted to 30 V. To ensure accuracy and repeatability, all MS data were corrected through an external reference (Lock Spray) employing leucine-enkephalin (Sigma Chemical), which presented a lock-mass ion at 556.2771 Da ($[M+H]^+$). MS/MS spectra of quasi-molecular ions were generated by applying different collision energies (CE) ranging from 20 to 30 eV to obtain variable characteristic ion fragments.

For the determination of elemental compositions and precise molecular weights from the mass spectra data, the MassLynx 4.1 data analysis software was utilized. The software was configured with a parent mass error tolerance of 5 ppm to ensure that the results were highly accurate. To guarantee the accuracy and reliability of the analytical methods and instruments, eight quality control (QC) samples were prepared by randomly extracting 20 μL from individual plasma samples. Throughout the entire analysis process, a QC sample and a blank sample were inserted after every six samples that were analyzed. Additionally, fourteen main ion peaks from the total ion chromatograms were selected for method validation.

### 2.6. Statistical analysis

The UHPLC-MS raw data, initially processed using MarkerLynx software, were converted into "mzML" format data with the assistance of ProteoWizard's MSConvertGUI software. Subsequently, we performed data preprocessing, which included peak extraction, peak matching, peak alignment, noise filtering, and retention time correction, utilizing the XCMS online cloud platform (https://xcmsonline.scripps.edu/). Following this preprocessing, the data underwent normalization via MetaboAnalyst 6.0 (http://www.MetaboAnalyst.ca/) and were subsequently imported into SIMCA software (Version 14.1, Umetrics AB, Umea, Sweden) for multivariate statistical analysis. Pareto scaling and mean-centering were employed for the normalization of all original data. Both principal component analysis (PCA) and orthogonal projection discriminate analysis (OPLS-DA) were utilized to distinguish between the NDDD and HL groups compared to the HC group. The validity and accuracy of the OPLS-DA model were confirmed through two hundred response permutation testings (RPT), with the intercepts of $Q^2Y$ for the corresponding model being $<0.05$, indicating no overfitting.

The predictive power of the model was evaluated by examining the closeness of the $R^2Y$ and $Q^2$ values to 1. Moreover, the difference between $R^2Y$ and $Q^2$ values had to be $< 0.3$, and the $Q^2$ value had to exceed 50%. To identify differential metabolites, an S-plot based on OPLS-DA was constructed, utilizing variable importance in projection (VIP) values to characterize the weighted coefficient of discrepant variables. Ions with VIP values exceeding 1 were considered highly significant. Statistical significance in differences between the HC group and disease groups was assessed through nonparametric tests and Student's t-test for two independent samples, conducted using SPSS 19.0 (IBM, Armonk, NY, USA). The threshold for statistical significance was set at $p < 0.05$.

MetaboAnalyst 6.0 was employed for multivariate statistical analysis. The generation of the volcano plot occurred within MetaboAnalyst 6.0 following logarithmic transformation and normalization of preprocessed ion peak intensities. The projection of the volcano plot primarily relied on the p-value and the fold-change value derived from the Student's t-test, comparing the disease groups to the HC group of corrected sample datasets. This plot visually represented the significant differences between each pair of sample data groups. Typically, variables with fold change (FC) values exceeding 1.2 or falling below 0.8 and a p-value of $<0.05$ on the volcano plot were identified as differential biomarkers [13]. The greater the differences, the further these points at the top location were from the center of the plot.

Subsequently, the characteristic ions meeting the criteria of VIP value $> 1$, p-value $<0.05$, and FC value $> 1.2$ or $<0.8$ were identified as potential biomarkers and further subjected to tandem mass spectrometry. The lipid metabolites were cross-referenced with the predicted/reported fragments from the human metabolome database (HMDB, http://www.hmdb.ca/), LIPID MAPS Lipidomics Gateway (http://www.lipidmaps.org/), and KEGG (https://www.kegg.jp/). To delve deeper into potential lipid biomarkers and the underlying pathological mechanisms of T2DM with dyslipidemia, the identified differential metabolites and the involved lipid metabolic pathways underwent evaluation through receiver operator characteristic (ROC) analysis, random forest analysis, and Pearson matrix correlation. The diagnostic potential of the identified biomarkers was assessed using the ROC curve, with emphasis on

**Table 1**
Characteristics of the study subjects across groups.

| Parameters | HC (n = 32) | NDDD (n = 36) | HL (n = 37) | *P* value | |
|---|---|---|---|---|---|
| | | | | NDDD *vs* HC | HL *vs* HC |
| Age (years) | 40.6 ± 8.25 | 50.6 ± 10.6 | 42.24 ± 8.7 | <0.0001 | 0.4566 |
| Sex, n (M/F) | 15/17 | 20/16 | 19/18 | −0.5354 | 0.2677 |
| FPG (mmol/L) | 4.52 ± 0.38 | 9.50 ± 0.74 | 4.66 ± 0.39 | <0.0001 | 0.0997 |
| 2hPBG (mmol/L) | 5.86 ± 0.84 | 15.52 ± 0.99 | 5.98 ± 0.64 | <0.0001 | 0.4298 |
| HbA1c (%) | 5.43 ± 0.28 | 9.66 ± 0.89 | 5.34 ± 0.30 | <0.0001 | 0.1699 |
| CHOL (mmol/L) | 4.30 ± 0.54 | 5.64 ± 0.86 | 5.80 ± 0.47 | <0.0001 | <0.0001 |
| TG (mmol/L) | 0.86 ± 0.37 | 2.38 ± 0.70 | 1.81 ± 0.60 | <0.0001 | <0.0001 |
| LDL-C (mmol/L) | 2.54 ± 0.47 | 3.33 ± 0.74 | 3.90 ± 0.41 | 0.0001 | <0.0001 |
| HDL-C (mmol/L) | 1.46 ± 0.21 | 1.04 ± 0.23 | 1.31 ± 0.25 | <0.0001 | 0.0102 |
| apoB (g/L) | 0.79 ± 0.14 | 1.13 ± 0.25 | 1.24 ± 0.12 | <0.0001 | <0.0001 |
| ALT (U/L) | 15.37 ± 8.96 | 27.84 ± 8.91 | 19.51 ± 7.95 | <0.0001 | 0.0167 |
| AST (U/L) | 18.06 ± 4.18 | 20.29 ± 5.69 | 19.70 ± 4.97 | 0.1049 | 0.1198 |
| CREA (μmol/L) | 73.85 ± 15.95 | 73.59 ± 16.79 | 73.19 ± 12.74 | 0.8877 | 0.9816 |

Data are shown as mean ± standard deviations.
NDDD: newly diagnosed T2DM with dyslipidemia; HL: hyperlipidemia; HC: health control; FPG: fasting plasma glucose; CHOL: total cholesterol; TG: triglycerides; LDL-C: low-density lipoprotein cholesterol; HDL-C: high-density lipoprotein cholesterol; HbA1c: hemoglobin A1c; apoB; apolipoprotein B; 2hPBG: 2-h postprandial blood glucose; ALT: alanine transaminase; AST: aspartate transaminase; CREA: creatinine.

the area under the curve (AUC) value, where AUC >0.7 indicated excellent diagnostic accuracy. Heat maps and related metabolite pathway analyses of the biomarkers were generated using MetaboAnalyst 6.0 and KEGG. Furthermore, both the random forest analysis and Pearson correlation analysis were conducted using MetaboAnalyst 6.0.

## 3. Results

### 3.1. Characteristics of the study subjects

In this study, a total of 36 NDDD subjects, 37 HL subjects, and 32 HC subjects participated. Table 1 summarizes the sociodemographic and clinical characteristics of the study subjects. In comparison to the HC group, the NDDD and HL groups exhibited higher levels of CHOL, TG, LDL-C, apo B, and ALT, while HDL-C levels were lower. Additionally, the NDDD group showed increased age, FPG, 2hPBG, and HbA1c, whereas these differences were not observed in the HL group. Gender, AST, and CREA were similar among the three groups. The duration of T2DM ranged from 1 to 12 months. Furthermore, the age of the NDDD participants did not demonstrate any significant correlation with HbA1c ($r = -0.065$, $p = 0.701$), FPG ($r = -0.288$, $p = 0.083$), 2hFBG ($r = -0.145$, $p = 0.443$), CHOL ($r = -0.067$, $p = 0.701$), TG ($r = 0.214$, $p = 0.218$), LDL-C ($r = 0.256$, $P = 0.138$), and apoB ($r = -0.017$, $p = 0.942$). This lack of correlation also held true for the HL group ($r = 0.196$, $p = 0.246$ for HbA1c; $r = -0.040$, $p = 0.812$ for FPG; $r = -0.067$, $p = 0.725$ for 2hFBG; $r = 0.145$, $p = 0.393$ for CHOL; $r = 0.280$, $p = 0.093$ for TG; $r = 0.078$, $p = 0.647$ for LDL-C; $r = -0.324$, $p = 0.151$ for apoB) and the HC group ($r = -0.215$, $p = 0.273$ for HbA1c; $r = -0.030$, $p = 0.864$ for FPG; $r = 0.027$, $p = 0.875$ for 2hFBG; $r = 0.202$, $p = 0.356$ for CHOL; $r = -0.187$, $p = 0.394$ for TG; $r = 0.034$, $p = 0.878$ for LDL-C; $r = -0.106$, $p = 0.543$ for apoB). The correlation analysis indicated that the significant differences in blood glucose and blood lipid levels between the NDDD and HC groups were not influenced by the relatively older age of the NDDD subjects.

### 3.2. Selecting and identifying differential lipid metabolites

The plasma samples from individual groups are depicted in the base peak positive ion UHPLC-MS chromatograms shown in Fig. S1. All quality control (QC) samples fell within two standard deviations (SDs) in the score plot, and 92.86% of the fourteen selected metabolite variables exhibited a relative standard deviation (RSD) of less than 30% (Fig. S2). These results demonstrate the stability and repeatability of the analytical method.

Fig. 1A–D presents the PCA plot and OPLS-DA score plot, revealing a significant separation between HC and NDDD subjects, as well as HC and HL subjects in positive ion mode. The cumulative $R^2X$, $R^2Y$, and $Q^2$ values of the OPLS-DA model were 0.304, 0.904, and 0.653 for the comparison between HC and NDDD subjects (Group 1), and 0.358, 0.907, and 0.865 for the comparison between HC and HL subjects (Group 2). These values indicate a good fit of the established models. The RPT test (Fig. 1E and F) was employed to confirm that the models did not over-fit, with $Q^2$ values of −0.334 and −0.409 in Group 1 and Group 2, affirming excellent predictability. As a result, 1256 variables were responsible for the cluster segregation among the three groups.

Fig. 1G and H displays the volcano plots. The x-axis represents the log2 fold change in the relative abundance of each metabolite in the NDDD and HL groups compared to the HC group, while the y-axis represents the statistical significance (negative log10 of the p-value of each metabolite). The points are divided into two different categories based on the combination of fold change and the p-value of each variable. The red points indicate a FC > 1.2 or <0.8 and a p-value <0.05, signifying a substantial fold change and high statistical significance. The differential lipid metabolites in the NDDD and HL groups exhibited significant alterations compared to the HC group. Ultimately, the differential variables were chosen based on their VIP values > 1, p-value <0.05, and FC values > 1.2 or <0.8.

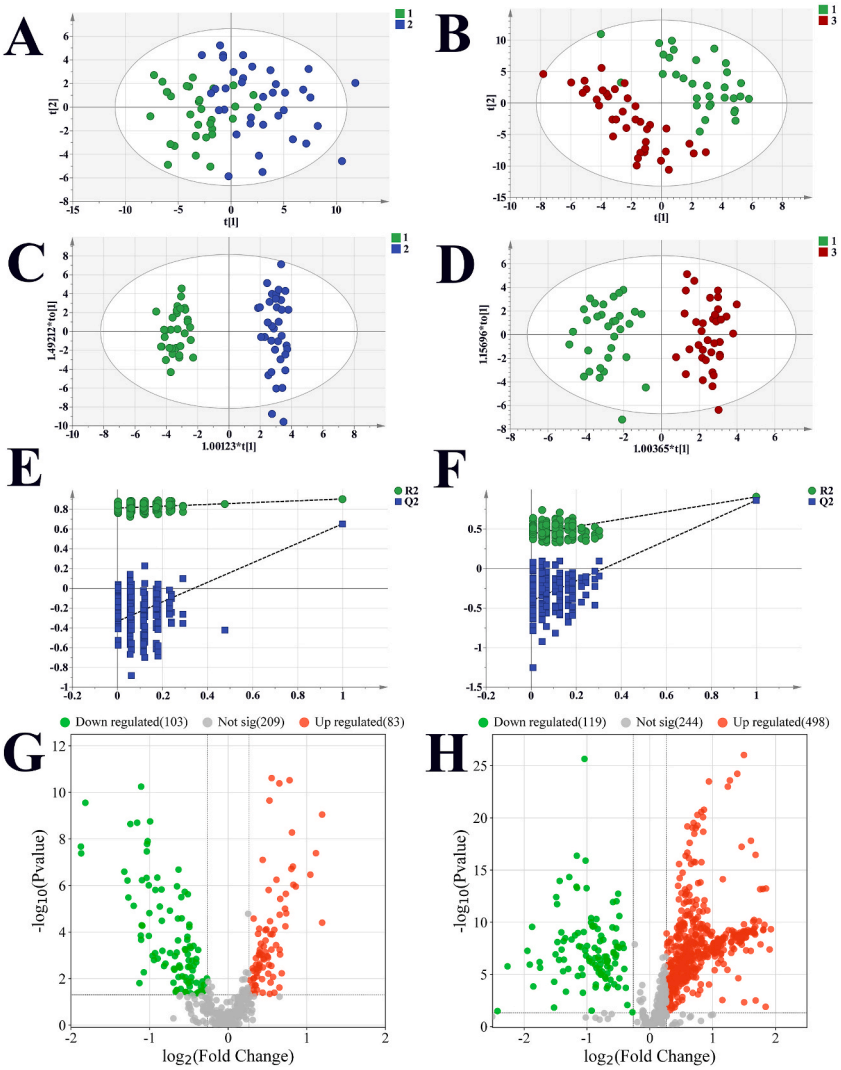


**Fig. 1.** PCA score plots (A, B) and OPLS-DA (C, D) score plots of lipidomics of plasma samples obtained from the HC vs NDDD group and HC vs HL group in positive ion mode. Permutation test plots of the OPLS-DA (E, F) in the (E) HC and NDDD groups (F) HC and HL groups. 1. HC group; 2. NDDD group; 3. HL group. Volcano plots were generated to select differential lipid metabolites between the HC and NDDD (G) and HL (H) groups. The x-axis represents log2 (fold change), and the y-axis represents -log10 (p-value). The red points indicate potential biomarkers with fold changes >1.2 or <0.8. (For interpretation of the references to colour in this figure legend, the reader is referred to the Web version of this article.)

The identified variables were further subjected to identification using MS and MS/MS data. The MassLynx software 4.1 was employed to deduce the elemental composition and accurate molecular weights of the differential lipid metabolites, with a margin of error for the *m/z* value of less than 5 ppm. In our previous study, UHPLC/Q-TOF-MS was used for a preliminary qualitative analysis of phospholipids in human plasma, resulting in the identification of 82 plasma lipids [14]. Detailed information on the identification processes of the differential lipid metabolites can be found in Supplementary Material 1. Our findings suggest that 15 lipid metabolites in Group 1 and 23 lipid metabolites in Group 2 could potentially serve as biomarkers for distinguishing between HC and NDDD, and HC and HL subjects, respectively.

In this study, the 15 lipid metabolites in Group 1 were categorized into five groups, including three lysophosphatidylcholines (LysoPCs), five phosphatidylcholines (PCs), one phosphatidylethanolamine (PE), five sphingomyelins (SMs), and one ceramide (Cer). Similarly, the 23 lipid biomarkers in Group 2 could be classified into three categories, consisting of four LysoPCs, sixteen PCs, and three SMs. Additional information on these lipid metabolites is provided in Tables 2 and 3.

### *3.3. Changes in screened lipid metabolites*

To provide an overview of the detailed levels of the 15 and 23 lipid metabolites in Group 1 and Group 2, a heat map was generated in Fig. 2A and B using Euclidean distances and Ward's algorithm for hierarchical clustering analysis. The heat map visually represents

**Table 2**
Detailed information of the lipid metabolites identified between the HC and NDDD groups.

| No. | $t_R$/min | Adduction | Mass ($m/z$) | | Mass accuracy (ppm) | Formula | VIP | FC | Trend[a] | Identification | HMDB ID |
|---|---|---|---|---|---|---|---|---|---|---|---|
| | | | Measured | Calculated | | | | | | | |
| 1 | 1.60 | $[M+H]^+$ | 520.3398 | 520.3403 | −1.0 | $C_{26}H_{50}NO_7P$ | 1.3806 | 1.2543 | ↓ | LysoPC(18:2/0:0) | HMDB0010386 |
| 2 | 2.10 | $[M+H]^+$ | 522.3581 | 522.3560 | 4.0 | $C_{26}H_{52}NO_7P$ | 1.2420 | 1.3465 | ↓ | LysoPC(18:1/0:0) | HMDB0010385 |
| 3 | 2.79 | $[M+H]^+$ | 524.3715 | 524.3716 | −0.2 | $C_{26}H_{54}NO_7P$ | 1.2105 | 1.4141 | ↓ | LysoPC(18:0/0:0) | HMDB0010384 |
| 4 | 6.18 | $[M+H]^+$ | 782.5731 | 782.5700 | 4.0 | $C_{44}H_{80}NO_8P$ | 1.0075 | 1.3271 | ↓ | PC(18:2/18:2) | HMDB0008138 |
| 5 | 7.48 | $[M+H]^+$ | 760.5839 | 760.5856 | −2.2 | $C_{42}H_{82}NO_8P$ | 1.1129 | 1.2461 | ↓ | PC(16:0/18:1) | HMDB0007971 |
| 6 | 7.86 | $[M+H]^+$ | 742.5768 | 742.5751 | 2.3 | $C_{42}H_{80}NO_7P$ | 1.1372 | 1.4526 | ↓ | PC(P-16:0/18:2) | HMDB0011211 |
| 7 | 8.17 | $[M+H]^+$ | 722.5154 | 722.5125 | 4.0 | $C_{41}H_{72}NO_7P$ | 1.2248 | 1.5732 | ↓ | PE(P-16:0/20:5) | HMDB0011354 |
| 8 | 8.23 | $[M+H]^+$ | 742.5723 | 742.5751 | −3.8 | $C_{42}H_{80}NO_7P$ | 1.3720 | 1.5817 | ↓ | PC(O-16:1/18:2) | HMDB0013413 |
| 9 | 9.04 | $[M+H]^+$ | 810.5995 | 810.6013 | −2.2 | $C_{46}H_{84}NO_8P$ | 1.1319 | 1.4315 | ↓ | PC(18:0/20:4) | HMDB0008048 |
| 10 | 10.76 | $[M+H]^+$ | 759.6383 | 759.6380 | 0.4 | $C_{43}H_{87}N_2O_6P$ | 1.0382 | 0.7870 | ↑ | SM(d18:1/20:0) | HMDB0012102 |
| 11 | 13.54 | $[M+H]^+$ | 787.6708 | 787.6693 | −1.1 | $C_{45}H_{91}N_2O_6P$ | 1.4224 | 0.7189 | ↑ | SM(d18:1/22:0) | HMDB0012103 |
| 12 | 13.97 | $[M+H]^+$ | 787.6685 | 787.6693 | −1.0 | $C_{45}H_{91}N_2O_6P$ | 1.4472 | 0.7580 | ↑ | SM(d18:0/22:1) | HMDB0012092 |
| 13 | 14.42 | $[M+H]^+$ | 801.6829 | 801.6850 | −2.6 | $C_{46}H_{93}N_2O_6P$ | 1.0259 | 0.7288 | ↑ | SM(d18:1/23:0) | HMDB0012105 |
| 14 | 15.21 | $[M+H]^+$ | 815.6976 | 815.7006 | −3.7 | $C_{47}H_{95}N_2O_6P$ | 1.1520 | 0.7099 | ↑ | SM(d18:1/24:0) | HMDB0011697 |
| 15 | 15.86 | $[M+H]^+$ | 650.6447 | 650.6451 | −0.6 | $C_{42}H_{83}NO_3$ | 2.0560 | 0.4639 | ↑ | Cer(d18:1/24:0) | HMDB0004956 |

VIP: variable importance in projection; FC: Fold Change of HC *vs* NDDD; [a] Compared with HC group, the change trend of potential lipid metabolites in the NDDD group, (↓) represent downregulated and (↑) represent upregulated. HMDB: HMDB database (http://www.hmdb.ca/).

**Table 3**
Detailed information of the lipid metabolites identified between the HC and HL groups.

| No. | $t_R$/min | Adduction | Mass ($m/z$) | | Mass accuracy (ppm) | Formula | VIP | FC | Trend[a] | Identification | HMDB ID |
|---|---|---|---|---|---|---|---|---|---|---|---|
| | | | Measured | Calculated | | | | | | | |
| 1 | 1.65 | $[M+Na]^+$ | 542.3212 | 542.3223 | −2.0 | $C_{26}H_{50}NO_7P$ | 1.7170 | 1.5198 | ↓ | LysoPC(18:2/0:0) | HMDB0010386 |
| 2 | 2.19 | $[M+H]^+$ | 544.3390 | 544.3403 | −2.4 | $C_{28}H_{50}NO_7P$ | 1.7182 | 1.4733 | ↓ | LysoPC(20:4/0:0) | HMDB0010395 |
| 3 | 2.41 | $[M+H]^+$ | 482.3605 | 482.3611 | −1.2 | $C_{24}H_{52}NO_6P$ | 2.0176 | 1.2785 | ↓ | PC(O-16:0/0:0) | / |
| 4 | 2.93 | $[M+H]^+$ | 546.3569 | 546.3560 | 1.6 | $C_{28}H_{52}NO_7P$ | 2.5555 | 1.2916 | ↓ | LysoPC(20:3/0:0) | HMDB0010393 |
| 5 | 3.38 | $[M+H]^+$ | 510.3543 | 510.3560 | −3.3 | $C_{25}H_{52}NO_7P$ | 1.0316 | 1.2785 | ↓ | LysoPC(17:0/0:0) | HMDB0012108 |
| 6 | 6.38 | $[M+H]^+$ | 730.5364 | 730.5387 | −3.1 | $C_{40}H_{76}NO_8P$ | 1.2735 | 0.6758 | ↑ | PC(14:0/18:2) | HMDB0007874 |
| 7 | 6.46 | $[M+H]^+$ | 806.5710 | 806.5700 | 1.2 | $C_{46}H_{80}NO_8P$ | 5.7662 | 1.2934 | ↓ | PC(18:2/20:4) | HMDB0008147 |
| 8 | 6.51 | $[M+H]^+$ | 756.5540 | 756.5543 | −0.4 | $C_{42}H_{78}NO_8P$ | 3.9877 | 1.2542 | ↓ | PC(16:1/18:2) | HMDB0008006 |
| 9 | 6.69 | $[M+H]^+$ | 804.5556 | 804.5543 | 1.6 | $C_{46}H_{78}NO_8P$ | 2.3245 | 1.3210 | ↓ | PC(16:1/22:6) | HMDB0008023 |
| 10 | 8.09 | $[M+H]^+$ | 766.5756 | 766.5751 | 0.7 | $C_{44}H_{80}NO_7P$ | 4.8927 | 1.2464 | ↓ | PC(P-16:0/20:4) | HMDB0011221 |
| 11 | 8.41 | $[M+H]^+$ | 806.5723 | 806.5700 | 2.9 | $C_{46}H_{80}NO_8P$ | 3.8319 | 1.3493 | ↓ | PC(16:0/22:6) | HMDB0007991 |
| 12 | 8.43 | $[M+H]^+$ | 768.5894 | 768.5907 | −1.7 | $C_{44}H_{82}NO_7P$ | 5.9058 | 1.3040 | ↓ | PC(O-16:0/20:4) | HMDB0013407 |
| 13 | 8.45 | $[M+H]^+$ | 742.5738 | 742.5745 | −1.0 | $C_{42}H_{80}NO_7P$ | 4.7351 | 1.3399 | ↓ | PC(O-16:1/18:2) | HMDB0013413 |
| 14 | 8.47 | $[M+H]^+$ | 780.5535 | 780.5543 | −1.0 | $C_{44}H_{78}NO_8P$ | 2.5146 | 1.2810 | ↓ | PC(16:1/20:4) | HMDB0008015 |
| 15 | 8.50 | $[M+H]^+$ | 794.6049 | 794.6064 | −1.9 | $C_{46}H_{84}NO_7P$ | 5.5490 | 1.3352 | ↓ | PC(P-18:0/20:4) | HMDB0011253 |
| 16 | 8.89 | $[M+H]^+$ | 701.5605 | 701.5598 | 1.0 | $C_{39}H_{77}N_2O_6P$ | 7.4711 | 0.4867 | ↑ | SM(d18:1/16:1) | HMDB0240613 |
| 17 | 9.30 | $[M+H]^+$ | 810.6015 | 810.6013 | 0.2 | $C_{46}H_{84}NO_8P$ | 11.0659 | 2.2246 | ↓ | PC(18:0/20:4) | HMDB0008048 |
| 18 | 10.13 | $[M+H]^+$ | 794.6058 | 794.6064 | −0.8 | $C_{46}H_{84}NO_7P$ | 2.8729 | 1.4734 | ↓ | PC(O-18:1/20:4) | HMDB0013432 |
| 19 | 10.19 | $[M+H]^+$ | 744.5905 | 744.5902 | 0.4 | $C_{42}H_{82}NO_7P$ | 2.7882 | 1.4599 | ↓ | PC(O-16:0/18:2) | HMDB0011151 |
| 20 | 10.57 | $[M+H]^+$ | 796.6199 | 796.6188 | 1.4 | $C_{46}H_{86}NO_7P$ | 3.8602 | 1.3769 | ↓ | PC(O-18:0/20:4) | HMDB0013420 |
| 21 | 10.61 | $[M+H]^+$ | 770.6060 | 770.6058 | 0.2 | $C_{44}H_{84}NO_7P$ | 2.7123 | 1.6599 | ↓ | PC(O-18:1/18:2) | HMDB0013425 |
| 22 | 11.52 | $[M+H]^+$ | 811.6694 | 811.6693 | 0.1 | $C_{47}H_{91}N_2O_6P$ | 6.0027 | 0.5335 | ↑ | SM(d18:2/24:1) | HMDB0240636 |
| 23 | 13.97 | $[M+H]^+$ | 813.6858 | 813.6850 | 1.0 | $C_{47}H_{93}N_2O_6P$ | 8.7982 | 0.4978 | ↑ | SM(d18:1/24:1) | HMDB0012107 |

VIP: variable importance in projection; FC: Fold Change of HC *vs* HL; [a] Compared with HC group, the change trend of potential lipid metabolites in the HL group, (↓) represent downregulated and (↑) represent upregulated. HMDB: Human metabolome database (http://www.hmdb.ca/).

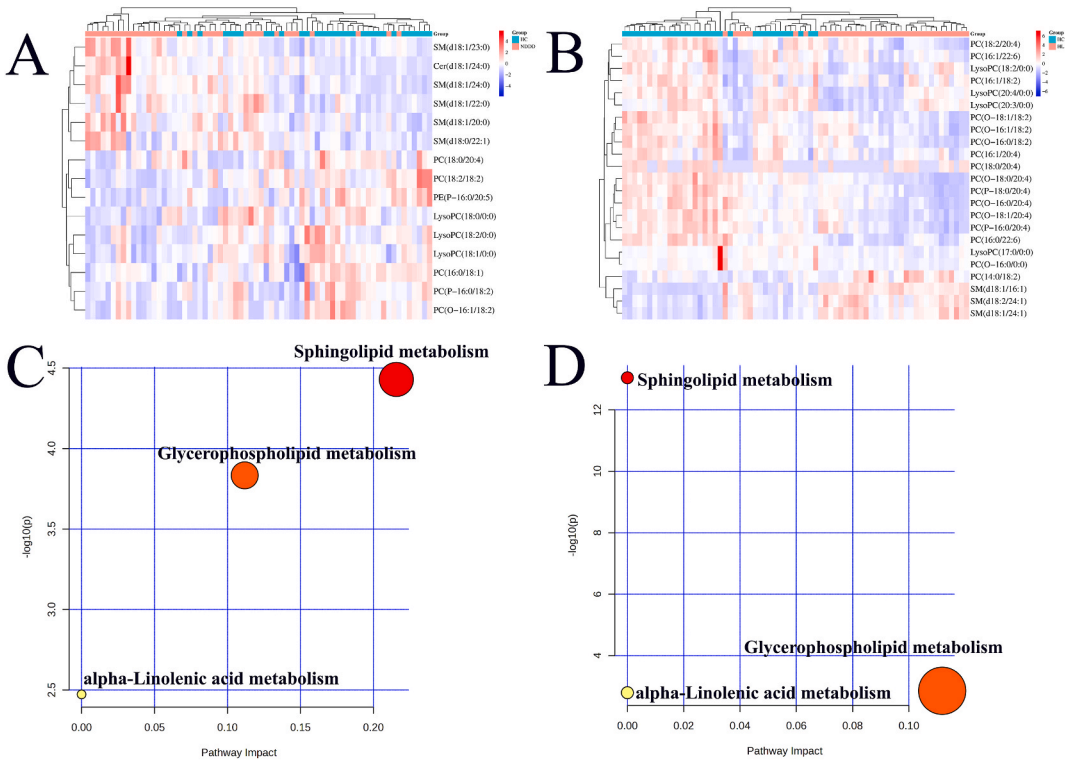


**Fig. 2.** Heat maps displaying significantly differential lipid biomarker levels between the HC and NDDD (A) and HL (B) groups. Metabolic pathway analysis of (C) 15 lipid metabolites in the HC and NDDD groups and (D) 23 lipid metabolites in the HC and HL groups was performed using MetaboAnalyst 6.0.

**Table 4**
Pathway analysis data with MetaboAnalyst 6.0 between HC and NDDD and HL groups.

| Gruop | Pathway Name | Match Status | Match Lipids | Raw *p* | -Log10 (*p*) | Holm *p* | FDR | Impact |
|---|---|---|---|---|---|---|---|---|
| HC *vs.* NDDD | Sphingolipid metabolism | 5/32 | SM(d18:1/20:0), SM(d18:1/22:0), SM(d18:1/23:0), SM(d18:1/24:0), Cer(d18:1/24:0) | 3.72E-05 | 4.4293 | 0.00018608 | 0.00018608 | 0.21576 |
| | Glycerophospholipid metabolism | 6/36 | LysoPC(18:2/0:0), LysoPC(18:1/0:0), LysoPC (18:0/0:0), PC(18:2/18:2), PC(16:0/18:1), PC (18:0/20:4) | 0.00014678 | 3.8333 | 0.00058714 | 0.00036696 | 0.11182 |
| | Arachidonic acid metabolism | 1/44 | PC(18:0/20:4) | 0.0033669 | 2.4728 | 0.010101 | 0.0033669 | 0 |
| | Linoleic acid metabolism | 1/5 | PC(18:2/18:2) | 0.0033669 | 2.4728 | 0.010101 | 0.0033669 | 0 |
| | alpha-Linolenic acid metabolism | 1/13 | PC(18:2/18:2) | 0.0033669 | 2.4728 | 0.010101 | 0.0033669 | 0 |
| HC *vs.* HL | Glycerophospholipid metabolism | 11/36 | LysoPC(18:2/0:0), LysoPC(20:4/0:0), LysoPC (20:3/0:0), LysoPC(17:0/0:0), PC(14:0/18:2), PC(18:2/20:4), PC(16:1/18:2), PC(16:1/22:6), PC(16:0/22:6), PC(16:1/20:4), PC(18:0/20:4) | 0.0013947 | 2.8555 | 0.0055789 | 0.0016066 | 0.11182 |
| | Sphingolipid metabolism | 1/32 | SM(d18:1/24:1) | 9.07E-14 | 13.042 | 4.53E-13 | 4.53E-13 | 0 |
| | Arachidonic acid metabolism | 3/44 | PC(18:2/20:4), PC(16:1/20:4), PC(18:0/20:4) | 0.0016066 | 2.7941 | 0.0055789 | 0.0016066 | 0 |
| | Linoleic acid metabolism | 2/5 | PC(18:2/20:4), PC(16:1/18:2) | 0.0016066 | 2.7941 | 0.0055789 | 0.0016066 | 0 |
| | alpha-Linolenic acid metabolism | 1/13 | PC(18:2/20:4) | 0.0016066 | 2.7941 | 0.0055789 | 0.0016066 | 0 |

the levels of lipid metabolites, ranging from low (blue) to intermediate (white) and high (red) in the disease groups. It is evident that the 15 lipid metabolites in Group 1 can be grouped into two distinct classes based on their levels. In the NDDD group, five SMs and Cer (d18:1/24:0) exhibited up-regulation, while three LysoPCs, five PCs, and one PE displayed down-regulation. Similarly, the HL group

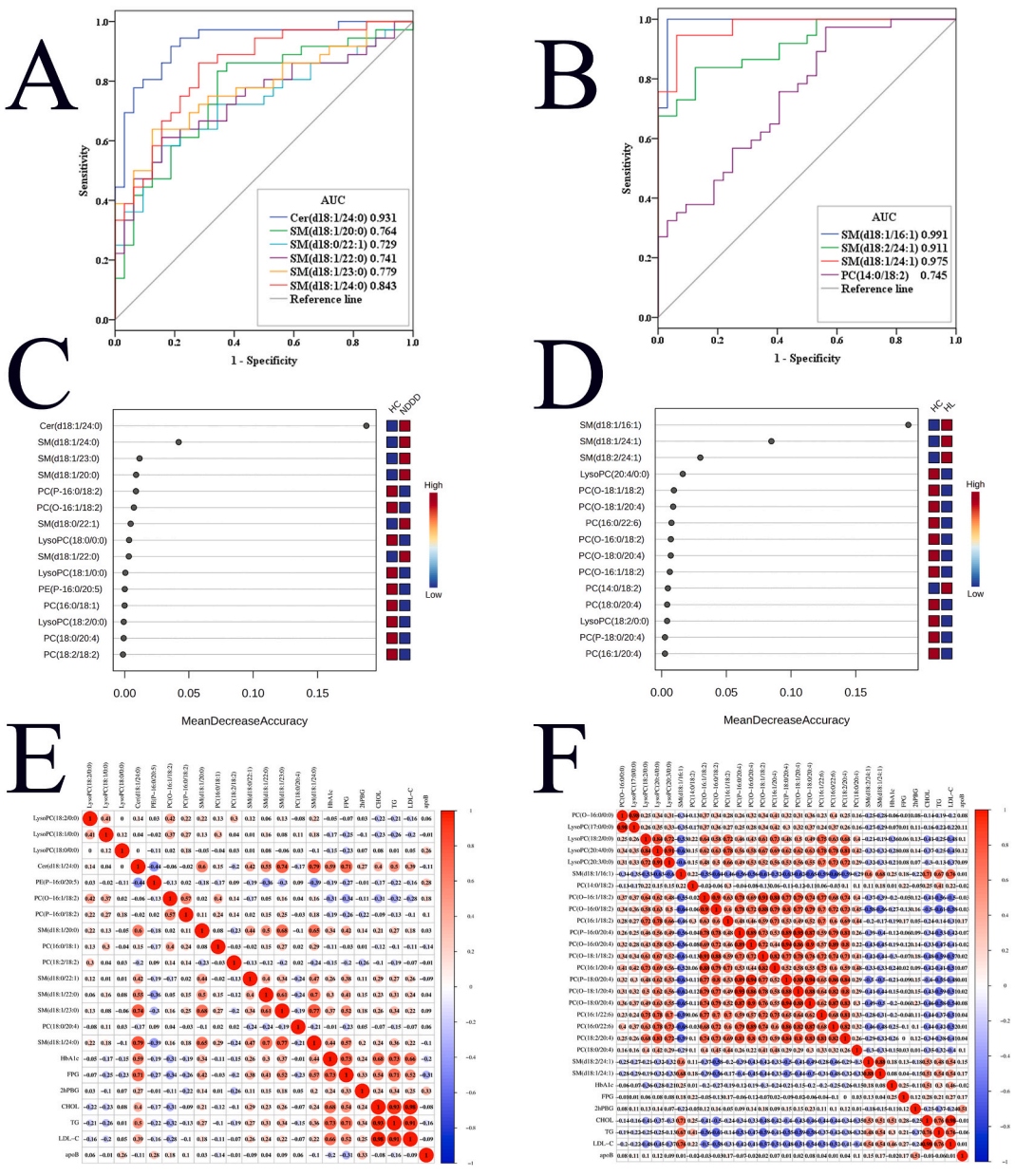


**Fig. 3.** ROC curves based on (A) 15 lipid biomarkers for the diagnosis of T2DM with dyslipidemia and (B) 23 lipid biomarkers for the diagnosis of HL. Random forest analysis of (C) 15 lipid biomarkers in the HC and NDDD groups and (D) 23 lipid biomarkers in the HC and HL groups based on mean decrease accuracy (MDA) values. Heat maps illustrating Pearson correlation coefficients between potential lipid biomarkers and clinical parameters of NDDD (E) and HL (F) subjects.

showed an increase in three SMs and PC(14:0/18:2), but a decrease in four LysoPCs and fifteen PCs.

### *3.4. Metabolic pathway analysis*

To gain insight into the contribution of lipid metabolites to the development of T2DM with dyslipidemia, the examination of relevant metabolic pathways was conducted using MetaboAnalyst 6.0. As depicted in Fig. 2C and D, five metabolic pathways, namely sphingolipid metabolism, glycerophospholipid metabolism, arachidonic acid metabolism, linoleic acid metabolism, and alpha-Linolenic acid metabolism, were identified in both Group 1 and Group 2. The results of the pathway analysis are presented in Table 4. When filter criteria were applied, with an impact value greater than 0.1 and a p-value less than 0.05, it was observed that sphingolipid metabolism and glycerophospholipid metabolism were found to be the pathways most significantly impacted by the development of T2DM with dyslipidemia. Additionally, a critical role in the development of hyperlipidemia was played by

glycerophospholipid metabolism.

### 3.5. Diagnostic value and correlation analysis of lipid biomarkers

To evaluate the effectiveness of lipid biomarkers in the plasma of Group 1 and Group 2, ROC curves were plotted and presented in Fig. 3A and B. Among the 15 lipid metabolites in Group 1, six yielded satisfactory diagnostic results, with an area under the ROC curve exceeding 0.7. Cer(d18:1/24:0), SM(d18:1/24:0), SM(d18:1/23:0), SM(d18:1/20:0), SM(d18:1/22:0), and SM(d18:0/22:1) were found to possess superior diagnostic efficiency compared to the remaining nine lipid metabolites in predicting T2DM with dyslipidemia. Among these, Cer(d18:1/24:0) and SM(d18:1/24:0) were identified as having the best diagnostic performance, with AUC values of 0.931 and 0.843, respectively. Furthermore, the diagnostic efficiency of SM(d18:1/16:1), SM(d18:1/24:1), SM(d18:2/24:1), and PC(14:0/18:2) exceeded that of the other 19 lipid metabolites for HL, with AUC values of 0.991, 0.975, 0.911, and 0.745, respectively.

To visually distinguish the NDDD and HL groups from the HC group and showcase the variability in lipid biomarker profiles, a random forest (RF) analysis was conducted using MetaboAnalyst 6.0. The potential lipid biomarkers with mean decrease accuracy (MDA) values are displayed in Fig. 3C and D. The top lipid metabolites, selected from the 15 and 23 potential lipid metabolites of Group 1 and Group 2, respectively, had the highest MDA values of 0.1880, 0.0421, 0.1907, and 0.0848. These lipid metabolites were Cer(d18:1/24:0), SM(d18:1/24:0), SM(d18:1/16:1), and SM(d18:1/24:1).

As depicted in Fig. 3E and F, Cer(d18:1/24:0) and SM(d18:1/24:0) exhibited significant positive correlations with FPG and HbA1c in Group 1, while SM(d18:1/16:1), SM(d18:1/24:1), and SM(d18:2/24:1) showed significant positive associations with LDL-C, CHOL, and TG in Group 2. These lipid biomarkers, which displayed positive correlations with traditional indicators of glucose and lipid metabolism, may help elucidate the process of T2DM associated with dyslipidemia.

## 4. Discussion

Lipidomics, employing UHPLC/Q-TOF-MS technology combined with multivariable analysis, was used for a comprehensive characterization of lipid profiles in NDDD and HL patients. Our study results reveal significant alterations in lipid metabolite profiles in both NDDD and HL groups when compared to the HC group. Notably, there was a substantial increase in the concentrations of Cer and SMs in the NDDD and HL groups, while LysoPCs, PCs, and PE exhibited decreased concentrations.

### 4.1. Sphingolipids

Sphingolipids are vital components of cell membranes, comprising SMs, glycosphingolipids, and Cers, and they play a crucial role in various bodily processes. Recent research indicates that obese patients have higher levels of Cers and SMs in their blood compared to those with normal weight, especially SMs with saturated acyl chains like C18:0, C20:0, C22:0, and C24:0 [15]. These specific SMs were found to be positively associated with homeostasis model assessment of insulin resistance (HOMA-IR), cholesterol (CHOL), and low-density lipoprotein cholesterol (LDL-C) [16]. Sokołowska et al. [17] demonstrated that autoimmune diabetes patients have elevated levels of SMs (C16:0, C16:1, C18:1, C18:3, and C20:4), and SMs (C18:0, C16:1, and C18:3) were notably increased in the T2DM group. Our findings support a strong link between elevated sphingolipid levels and the onset of type 2 diabetes with dyslipidemia.

In this study, we observed significant increases in Cer(d18:1/24:0), SM(d18:1/24:0), SM(d18:1/23:0), SM(d18:1/20:0), SM(d18:1/22:0), and SM(d18:0/22:1) levels in T2DM patients with dyslipidemia. Furthermore, patients with hyperlipidemia exhibited substantial increases in SM(d18:1/16:1), SM(d18:1/24:1), and SM(d18:2/24:1) levels. Notably, Cer(d18:1/24:0) and SM(d18:1/24:0) exhibited significant positive correlations with fasting blood glucose (FBG) and hemoglobin A1c (HbA1c), while SM(d18:1/16:1), SM (d18:1/24:1), and SM(d18:2/24:1) displayed positive correlations with LDL-C, CHOL, and triglycerides (TG). These lipid biomarkers hold promise for potential clinical use in diagnosing, monitoring progress, and evaluating therapeutic effectiveness in patients with T2DM and dyslipidemia or hyperlipidemia.

In recent years, plasma SMs and Cers have been increasingly utilized as indicators to predict the progression of various chronic diseases. For instance, elevated levels of Cer(d18:1/16:0), Cer(d18:1/18:0), Cer(d18:1/20:0), Cer(d18:1/22:0), Cer(d18:1/24:0), and Cer(d18:1/24:1) have been associated with chronic kidney disease, both with and without coronary artery disease [18]. Additionally, Cer(d16:1/24:0), Cer(d18:1/16:0), SM(d16:1/22:0), and HexCer(d18:1/18:0) have shown strong positive associations with Alzheimer's disease [19]. Recent research has revealed significant disruptions in ceramide and sphingomyelin balance in prediabetic and T2DM patients [20]. The disturbance observed in the NDDD group may result from the accumulation of sphingolipids, leading to the development of endoplasmic reticulum stress (ERS), mitochondrial dysfunction, transcriptional inhibition of insulin genes, and ultimately, apoptosis of pancreatic β cells [21,22].

### 4.2. Glycerophospholipids

Glycerophospholipids (GPs) constitute the primary component of cell membranes, including PCs, LysoPCs, PEs, and others. Previous studies have reported a significant decrease in LysoPC concentrations in patients with impaired FPG, T2DM, and in animal models of obesity or IR. García-Fontana et al. [23] demonstrated that levels of PCs, LysoPCs, and LysoPEs in serum were notably reduced in T2DM patients, especially those with cardiovascular disease. More recently, a prospective cohort study revealed that black

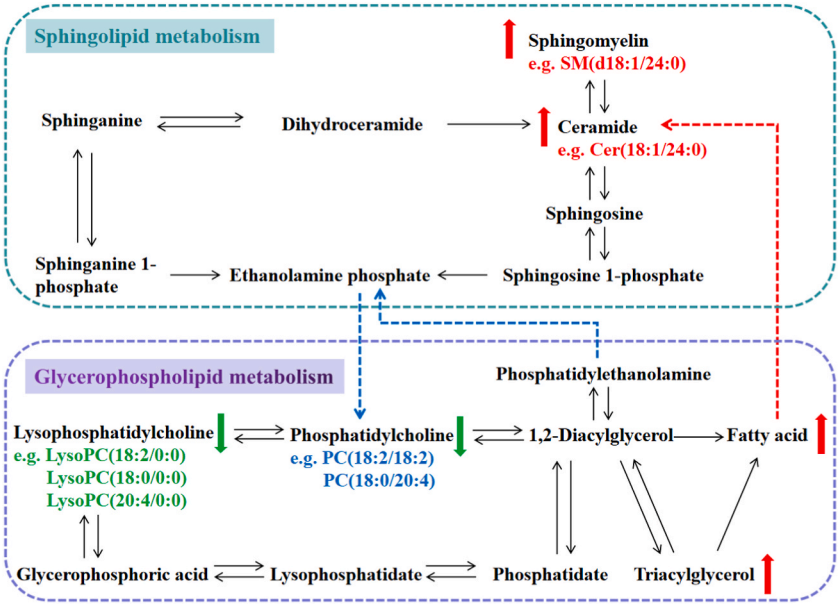


**Fig. 4.** The metabolic pathways network of potential biomarkers from KEGG. The red upward arrow and blue downward arrow indicate that potential biomarkers are upregulated or downregulated in the NDDD and HL groups, respectively. (For interpretation of the references to colour in this figure legend, the reader is referred to the Web version of this article.)

South African women with normal glucose tolerance (NGT), who developed T2DM (NGT-T2DM group) over a 13-year period, had lower levels of LPC(C18:2) compared to those who maintained NGT (NGT-NGT group) [24]. The longitudinal METSIM study also found a negative association between LysoPC(18:2) levels and hyperglycemia and T2DM risk [25]. Another study demonstrated that changes in LysoPC levels over one year were inversely related to the risk of T2DM in a Mediterranean population at high cardiovascular risk [26]. Our findings align with the aforementioned research.

In this study, we observed lower levels of LysoPC(18:2/0:0), LysoPC(18:1/0:0), LysoPC(18:0/0:0), LysoPC(20:4/0:0), LysoPC (20:3/0:0), and LysoPC(17:0/0:0) in patients with T2DM-associated dyslipidemia and hyperlipidemia. These showed a negative association with blood glucose levels (HbA1c and FPG) and blood lipid indexes (LDL-C, CHOL, TG). Several studies have indicated that LysoPCs can lower blood glucose levels by increasing GLUT4 expression on adipocyte membranes and activating the orphan G-protein-coupled receptor GPR119 [27–29]. PCs can be hydrolyzed into LysoPCs and free fatty acids (FFAs) by phospholipase A2 (PLA2). Prolonged hyperglycemia can accelerate PC degradation by activating protein kinase C and enhancing PLA2 activity [30]. It appears that nearly all PCs experience a significant decrease in the NDDD and HL groups. PCs can reduce LDL-C and TC levels, enhance pancreatic function, restore pancreatic β cells, stimulate insulin secretion, and improve insulin sensitivity. PC deficits can affect β cell function and lead to insulin secretion disorders [31].

Lipid metabolism disorder is a crucial risk factor for elevated blood glucose levels. Core receptors for de novo lipogenesis, such as sterol regulatory element binding protein 1c (SREBP-1c), carbohydrate response element binding protein (ChREBP), and liver X receptor (LXRα), play important roles in the insulin signaling pathway. Insulin activates de novo lipogenesis through phosphatidylinositol 3-kinase (PI3K)-mediated regulation of fatty acid synthase (FAS) and acetyl-CoA carboxylase 1 (ACC1) expression [32]. Insulin inhibits lipolysis and the release of FFAs in adipocytes, while insulin resistance in adipocytes enhances lipolysis, leading to elevated FFAs in the bloodstream. FFAs can inhibit insulin production and secretion by activating endoplasmic reticulum stress (ERS), reducing the expression of the anti-apoptotic factor B-cell CLL/lymphoma 2 (Bcl-2), and triggering β cell apoptosis [33].

Based on current research, we hypothesize that elevated levels of circulating FFAs can stimulate the de novo synthesis of ceramides and sphingosines under high-fat conditions, thereby promoting the biosynthesis of Cers and SMs. Our speculation is supported by a literature review [34,35], which indicates a positive correlation between the levels of ceramides and sphingosines in plasma and the total content of FFAs in plasma. Under high-glucose conditions, increased phospholipase A2 (PLA2) activity promotes the hydrolysis of LysoPCs and PCs, resulting in a significant reduction in their plasma levels and the production of abundant FFAs. These FFAs further stimulate the substantial generation of Cers, ultimately leading to the apoptosis of pancreatic β cells. The constructed metabolic pathways network of potential biomarkers is depicted in Fig. 4.

Currently, the molecular mechanism underlying T2DM caused by disturbances in lipid biomarkers remains unclear, and pharmacological studies based on lipid-related signaling pathways require further investigation. This study lays a fundamental foundation for research into the pathological mechanisms and potential therapeutic targets for the treatment of T2DM with dyslipidemia.

However, this study has several limitations. It was conducted at a single center, and future research should consider implementing multi-center studies to enhance the reproducibility and reliability of the conclusions. Additionally, the sample size was relatively small, which may restrict the generalizability of the findings. Furthermore, there was no validation or quantitative analysis of the

biomarkers conducted, and additional studies should address this issue.

## 5. Conclusions

In this study, 15 differential lipid biomarkers were identified in Chinese T2DM patients with dyslipidemia, and 23 were identified in those with hyperlipidemia. Sphingolipid metabolism and glycerophospholipid metabolism were found to be the major contributors to the development of T2DM with dyslipidemia. Valuable insights into risk prediction and the potential metabolic mechanisms in Chinese T2DM patients with dyslipidemia were provided by these findings. Further research will involve the exploration of the signaling pathways and therapeutic targets associated with these lipid biomarkers.

## Ethical approval

Ethical approval was granted by the Ethics committee of the Second Affiliated Hospital of Guangzhou Medical University (No: 2020-hs-07).

## Funding

This study was supported by the Projects of Traditional Chinese Medicine Bureau of Guangdong Province (No. 20221242), the Special Fund for Hospital Pharmaceutical Research of Guangdong Province Hospital Association (No. YXKY202201), the Medical Scientific Research Foundation of Guangdong Province (No. A2023420), the Project of Traditional Chinese Medicine and Pharmacology of Guangzhou Municipal Health Commission (No. 20222A011017), and the Guangzhou three-level Chinese medicine Studio Construction Project of Guangzhou Health Bureau (No. 2023077).

## Data availability

Data will be made available on request.

## CRediT authorship contribution statement

**Xunlong Zhong:** Writing – original draft, Methodology, Investigation, Conceptualization. **Chang Xiao:** Validation, Formal analysis. **Ruolun Wang:** Supervision. **Yunfeng Deng:** Visualization, Software. **Tao Du:** Investigation. **Wangen Li:** Investigation. **Yanmei Zhong:** Writing – review & editing, Project administration, Data curation. **Yongzhen Tan:** Resources, Funding acquisition, Conceptualization.

## Declaration of competing interest

The authors declare that they have no known competing financial interests or personal relationships that could have appeared to influence the work reported in this paper.

## Appendix B. Supplementary data

Supplementary data to this article can be found online at https://doi.org/10.1016/j.heliyon.2024.e26326.

## References

[1] H. Sun, P. Saeedi, S. Karuranga, M. Pinkepank, K. Ogurtsova, B.B. Duncan, C. Stein, A. Basit, J.C.N. Chan, J.C. Mbanya, et al., IDF Diabetes Atlas: Global, regional and country-level diabetes prevalence estimates for 2021 and projections for 2045, Diabetes Res. Clin. Pract. 183 (2022) 109119, https://doi.org/10.1016/j.diabres.2021.109119.

[2] Y. Xu, L.M. Wang, J. He, Y.F. Bi, M. Li, T.G. Wang, L.H. Wang, Y. Jiang, M. Dai, J.L. Lu, et al., 2010 China Noncommunicable disease Surveillance group. Prevalence and control of diabetes in Chinese adults, JAMA 310 (2013) 948–959, https://doi.org/10.1001/jama.2013.168118.

[3] J.I. Morton, P.A. Lazzarini, K.R. Polkinghorne, B. Carstensen, D.J. Magliano, J.E. Shaw, The association of attained age, age at diagnosis, and duration of type 2 diabetes with the long-term risk for major diabetes-related complications, Diabetes Res. Clin. Pract. 190 (2022) 110022, https://doi.org/10.1016/j.diabres.2022.110022.

[4] D. Duan, A.P. Kengne, J.B. Echouffo-Tcheugui, Screening for diabetes and prediabetes, Endocrinol Metab. Clin. N. Am. 50 (2021) 369–385, https://doi.org/10.1016/j.ecl.2021.05.002.

[5] A. Mousa, N. Naderpoor, N. Mellett, K. Wilson, M. Plebanski, P.J. Meikle, B. de Courten, Lipidomic profiling reveals early-stage metabolic dysfunction in overweight or obese humans, Biochim. Biophys. Acta Mol. Cell Biol. Lipids 1864 (2019) 335–343, https://doi.org/10.1016/j.bbalip.2018.12.014.

[6] B. Verges, Pathophysiology of diabetic dyslipidaemia: where are we? Diabetologia 58 (2015) 886–899, https://doi.org/10.1007/s00125-015-3525-8.

[7] P.J. Meikle, G. Wong, C.K. Barlow, B.A. Kingwell, Lipidomics: potential role in risk prediction and therapeutic monitoring for diabetes and cardiovascular disease, Pharmacol. Ther. 143 (2014) 12–23, https://doi.org/10.1016/j.pharmthera.2014.02.001.

[8] M. Mujammami, S.M. Aleidi, A.Z. Buzatto, A. Alshahrani, R.H. AlMalki, H. Benabdelkamel, M. Al Dubayee, L. Li, A. Aljada, A.M. Abdel Rahman, Lipidomics profiling of Metformin-induced changes in obesity and type 2 diabetes mellitus: insights and biomarker potential, Pharmaceuticals 16 (2023) 1717, https://doi.org/10.3390/ph16121717.

[9] A. Villasanta-Gonzalez, M. Mora-Ortiz, J.F. Alcala-Diaz, L. Rivas-Garcia, J.D. orres-Peña, A. Lopez-Bascon, M. Calderon-Santiago, A.P. Arenas-Larriva, F. Priego-Capote, M.M. Malagon, et al., Plasma lipidic fingerprint associated with type 2 diabetes in patients with coronary heart disease: CORDIOPREV study, Cardiovasc, Diabetologe 22 (2023) 199, https://doi.org/10.1186/s12933-023-01933-1.

[10] T. Suvitaival, I. Bondia-Pons, L. Yetukuri, P. Pöhö, J.J. Nolan, T. Hyötyläinen, J. Kuusisto, M. Orešič, Lipidome as a predictive tool in progression to type 2 diabetes in Finnish men, Metabolism 78 (2018) 1–12, https://doi.org/10.1016/j.metabol.2017.08.014.

[11] C. Zusi Amantovani, G. Lunardi, S. Bonapace, G. Lippi, C. Maffeis, G. Targher, Association between KLF6 rs3750861 polymorphism and plasma ceramide concentrations in post-menopausal women with type 2 diabetes, Nutr. Metabol. Cardiovasc. Dis. 32 (2022) 1283–1287, https://doi.org/10.1016/j.numecd.2022.01.037.

[12] W. Jia, J. Weng, D. Zhu, L. Ji, J. Lu, Z. Zhou, D. Zou, L. Guo, Q. Ji, L. Chen, et al., Chinese Diabetes Society, Standards of medical care for type 2 diabetes in China 2019, Diabetes Metab. Res. Rev. 35 (2019) e3158, https://doi.org/10.1002/dmrr.3158.

[13] H. Mao, H. Huang, R. Zhou, J. Zhu, J. Yan, H. Jiang, L. Zhang, High preoperative blood oxaloacetate and 2-aminoadipic acid levels are associated with postoperative delayed neurocognitive recovery, Front. Endocrinol. 14 (2023) 1212815, https://doi.org/10.3389/fendo.2023.1212815.

[14] X.L. Zhong, R.L. Wang, L.S. Chen, Y.M. Zhong, Rapid analysis and determination of the fragmentation regularity of phospholipids in human plasma based on UHPLC/Q-TOF-MS, Acta Pharm. Sin. 57 (2022) 3214–3222, https://doi.org/10.16438/j.0513-4870.2022-0627.

[15] K. Ohtsubo, S. Takamatsu, C. Gao, H. Korekane, T.M. Kurosawa, N. Taniguchi, N-Glycosylation modulates the membrane sub-domain distribution and activity of glucose transporter 2 in pancreatic beta cells, Biochem, Biophys. Res. Commun 434 (2013) 346–351, https://doi.org/10.1016/j.bbrc.2013.03.076.

[16] M. Martínez-Ramírez, M. Madero, G. Vargas-Alarcón, J. Vargas-Barrón, J.M. Fragoso, J.M. Rodríguez-Pérez, C. Martínez-Sánchez, H. González-Pacheco, R. Bautista-Pérez, E. Carreón-Torres, et al., HDL-sphingomyelin reduction after weight loss by an energy-restricted diet is associated with the improvement of lipid profile, blood pressure, and decrease of insulin resistance in overweight/obese patients, Clin. Chim. Acta 454 (2016) 77–81, https://doi.org/10.1016/j.cca.2015.12.039.

[17] E. Sokołowska, H. Car, A. Fiedorowicz, M. Szelachowska, A. Milewska, N. Wawrusiewicz-Kurylonek, P. Szumowski, E. Krzyzanowska-Grycel, A. Popławska-Kita, M. Zendzian-Piotrowska, et al., Sphingomyelin profiling in patients with diabetes could be potentially useful as differential diagnostics biomarker: a pilot study, Adv. Med. Sci. 67 (2022) 250–256, https://doi.org/10.1016/j.advms.2022.06.001.

[18] A. Mantovani, G. Lunardi, S. Bonapace, C. Dugo, A. Altomari, G. Molon, A. Conti, C. Bovo, R. Laaksonen, C.D. Byrne, et al., Association between increased plasma ceramides and chronic kidney disease in patients with and without ischemic heart disease, Diabetes Metab. 47 (2021) 101152, https://doi.org/10.1016/j.diabet.2020.03.003.

[19] X.Y. Chua, F. Torta, J.R. Chong, N. Venketasubramanian, S. Hilal, M.R. Wenk, C.P. Chen, T.V. Arumugam, D.R. Herr, M.K.P. Lai, Lipidomics profiling reveals distinct patterns of plasma sphingolipid alterations in Alzheimer's disease and vascular dementia, Alzheimer's Res. Ther. 15 (2023) 214, https://doi.org/10.1186/s13195-023-01359-7.

[20] J. Yang, M. Wang, D. Yang, H. Yan, Z. Wang, D. Yan, N. Guo, Integrated lipids biomarker of the prediabetes and type 2 diabetes mellitus Chinese patients, Front. Endocrinol. 13 (2023) 1065665, https://doi.org/10.3389/fendo.2022.1065665.

[21] H. Yaribeygi, S. Bo, M. Ruscica, A. Sahebkar, Ceramides and diabetes mellitus: an update on the potential molecular relationships, Diabet. Med. 37 (2020) 11–19, https://doi.org/10.1111/dme.13943.

[22] M. Yano, K. Watanabe, T. Yamamoto, K. Ikeda, T. Senokuchi, M. Lu, T. Kadomatsu, H. Tsukano, M. Ikawa, M. Okabe, et al., Mitochondrial dysfunction and increased reactive oxygen species impair insulin secretion in sphingomyelin synthase 1-null mice, J. Biol. Chem. 286 (2011) 3992–4002, https://doi.org/10.1074/jbc.M110.179176.

[23] B. García-Fontana, S. Morales-Santana, C. Díaz Navarro, P. Rozas-Moreno, O. Genilloud, F. Vicente Pérez, J. Pérez del Palacio, M. Muñoz-Torres, Metabolomic profile related to cardiovascular disease in patients with type 2 diabetes mellitus: a pilot study, Talanta 148 (2016) 135–143, https://doi.org/10.1016/j.talanta.2015.10.070.

[24] Y. Zeng, A. Mtintsilana, J.H. Goedecke, L.K. Micklesfield, T. Olsson, E. Chorell, Alterations in the metabolism of phospholipids, bile acids and branched-chain amino acids predicts development of type 2 diabetes in black South African women: a prospective cohort study, Metabolism 95 (2019) 57–64, https://doi.org/10.1016/j.metabol.2019.04.001.

[25] T. Suvitaival, I. Bondia-Pons, L. Yetukuri, P. Pöhö, J.J. Nolan, T. Hyötyläinen, J. Kuusisto, M. Orešič, Lipidome as a predictive tool in progression to type 2 diabetes in Finnish men, Metabolism 78 (2018) 1–12, https://doi.org/10.1016/j.metabol.2017.08.014.

[26] C. Razquin, E. Toledo, C.B. Clish, M. Ruiz-Canela, C. Dennis, D. Corella, C. Papandreou, E. Ros, R. Estruch, M. Guasch-Ferre, et al., Plasma lipidomic profiling and risk of type 2 diabetes in the PREDIMED trial, Diabetes Care 41 (2018) 2617–2624, https://doi.org/10.2337/dc18-0840.

[27] S.H. Law, M.L. Chan, G.K. Marathe, F. Parveen, C.H. Chen, L.Y. Ke, An Updated review of lysophosphatidylcholine metabolism in human diseases, Int. J. Mol. Sci. 20 (2019) 1149, https://doi.org/10.3390/ijms20051149.

[28] K. Yea, J. Kim, J.H. Yoon, T. Kwon, J.H. Kim, B.D. Lee, H.J. Lee, S.J. Lee, J.I. Kim, T.G. Lee, et al., Lysophosphatidylcholine activates adipocyte glucose Uptake and lowers blood glucose levels in Murine models of diabetes, J. Biol. Chem. 284 (2009) 33833–33840, https://doi.org/10.1074/jbc.M109.024869.

[29] T. Soga, T. Ohishi, T. Matsui, T. Saito, M. Matsumoto, J. Takasaki, S. Matsumoto, M. Kamohara, H. Hiyama, S. Yoshida, et al., Lysophosphatidylcholine enhances glucose-dependent insulin secretion via an orphan G-protein-coupled receptor, Biochem. Biophys. Res. Commun. 326 (2005) 744–751, https://doi.org/10.1016/j.bbrc.2004.11.120.

[30] Y. Zhai, X. Cao, S. Liu, Y. Shen, The diagnostic value of lipoprotein-associated phospholipase A2 in early diabetic nephropathy, Ann. Med. 55 (2023) 2230446, https://doi.org/10.1080/07853890.2023.2230446.

[31] P. Canning, B.A. Kenny, V. Prise, J. Glenn, M.H. Sarker, N. Hudson, M. Brandt, F.J. Lopez, D. Gale, P.J. Luthert, et al., Lipoprotein-associated phospholipase A2 (Lp-PLA2) as a therapeutic target to prevent retinal vasopermeability during diabetes, Proc. Natl. Acad. Sci. U.S.A. 113 (2016) 7213–7218, https://doi.org/10.1073/pnas.1514213113.

[32] G.H. Zhang, J.X. Xu, Y. Chen, P.H. Guo, Z.L. Qiao, R.F. Feng, S.E. Chen, J.L. Bai, S.D. Huo, Z.R. Ma, ChREBP and LXRα mediate synergistically lipogenesis induced by glucose in porcine adipocytes, Gene 565 (2015) 30–38, https://doi.org/10.1016/j.gene.2015.03.057.

[33] S.A. Litwak, J.A. Wali, E.G. Pappas, H. Saadi, W.J. Stanley, L.C. Varanasi, T.W. Kay, H.E. Thomas, E.N. Gurzov, Lipotoxic stress induces pancreatic β-cell apoptosis through modulation of bcl-2 proteins by the ubiquitin-proteasome system, J. Diabetes Res. 2015 (2015) 280615, https://doi.org/10.1155/2015/280615.

[34] P. Zabielski, A.U. Błachnio-Zabielska, B. Wójcik, A. Chabowski, J. Górski, Effect of plasma free fatty acid supply on the rate of ceramide synthesis in different muscle types in the rat, PLoS One 12 (2017) e0187136, https://doi.org/10.1371/journal.pone.0187136.

[35] B. Chaurasia, C.L. Talbot, S.A. Summers, Adipocyte ceramides-the Nexus of Inflammation and metabolic disease, Front. Immunol. 11 (2020) 576347, https://doi.org/10.3389/fimmu.2020.576347.